Charge separation at a plasma edge in the presence of a density gradient

M. Shoucri, E. Pohn,[a] G. Knorr,[b] P. Bertrand,[c] G. Kamelander,[a] G. Manfredi,[c] and A. Ghizzo[c]
Centre Canadien de fusion Magnétique, Varennes, Québec, J3X 1S1, Canada

(Received 17 December 1999; accepted 11 February 2000)

A fully kinetic code for ions [one dimensional (1-D) in space, and using the three velocity dimensions in velocity space] is used to study the problem of the formation of a charge separation with the self-consistent electric field in a plasma in the presence of a density gradient. Electrons are treated using an adiabatic law. Graphical results are presented which follow the formation of a 1-D steady state showing the formation of an oscillating positive potential bump toward the edge of the plasma. These oscillations are closely associated with the gyration of the ions. It is also shown that the presence of a small fraction of impurity ions at the plasma edge can have a significant effect on the rapid buildup of the potential at the edge, and in increasing the charge separation and the associated electric field at the edge, in comparison to the case when no impurity ions are included. The present results show the importance of a kinetic solution to the problem of the equilibrium electric field and charge separation in the presence of a density gradient, and point to the important role played by the finite ions' gyroradius and the important contribution of impurity ions in this case.
© *2000 American Institute of Physics.* [S1070-664X(00)03906-9]

I. INTRODUCTION

The problem of the formation of a charge separation in a plasma in the presence of a steep density gradient is of major importance in many physical problems. In tokamak physics, it is the central problem in the physics associated with the high confinement mode (H mode) and the reversed shear equilibria. In a previous work,[1] we presented a study of this problem using a two-dimensional gyro-kinetic code for the ions, with electrons following an adiabatic law. The gyro-kinetic code showed the formation of a stable (for the parameters studied) one-dimensional (1-D) equilibrium, with an effective charge separation which resulted from the conjugate or simultaneous effect of the finite ions' gyroradius and the presence of the steep density gradient. In this case the electron density changes rapidly over an ion orbit size and the electrons cannot exactly compensate the ions charge along the gradient, due to finite ions' gyroradius. This effect is especially important for large values of ρ_i/λ_{De} (ρ_i is the ions' gyroradius and λ_{De} the Debye length).

We complement the results published in Ref. 1 with the present work, which studies the same problem using a fully kinetic 1-D Eulerian Vlasov code for the ions (one spatial dimension and three velocity dimensions). The numerical solution is effected by integrating the Vlasov equation along the characteristics, which are the exact ion orbits, using a method of fractional steps (see Ref. 2). The gyro-kinetic approximation used in Ref. 1 imposes some limitations on the scale lengths of the parameters used. It also involves an averaging in the direction perpendicular to the magnetic field over a distribution function which is assumed to be a Maxwellian with constant temperature. As we shall see in the present results, this is not generally the case, especially for the large gyro-orbit impurity ions which give an important contribution to the charge at the edge. The combined effect due to the existence of a potential and an electric field at the edge, with the gyration in velocity space across the magnetic field, will generally distort the distribution functions from a Maxwellian. In addition, the fully kinetic code allows us to study the edge localized oscillations associated with the gyration of the ions. The kinetic code also confirms the results of Ref. 1 that small fractions of impurity ions can add a significant contribution to the charge and electric field in the presence of a gradient, and gives a more accurate description of the kinetic of the ions and of the impurities. Also, the present simulation follows the formation and buildup of the potential at the edge and shows how the presence of impurity ions contribute to a significant acceleration of the fast buildup of the potential and charge separation at the edge.

Attention has long been paid to the important role played by small fractions of impurity ions in the peripheral region of a tokamak plasma, both in the excitation of modes driven by the density gradient which control the energy transport in the plasma edge,[3,4] and in the fact that small quantities of impurity ions greatly enhance the radiation losses in the plasma.[5] Preliminary results with the present kinetic code, which includes the important effect of the ions gyroradius, have been presented in Ref. 6. The present results point out the importance of the finite ions gyroradius effect in many problems of plasma–wall transition with steep plasma parameters. Eulerian Vlasov codes, having a low noise level, offer a powerful tool for the study of these problems.

II. THE PERTINENT EQUATIONS

We approximate the plasma edge in the toroidal geometry by a slab. We consider a 1-D slab geometry, the y di-

[a]Also at: Forschungszentrum Seibersdorf, Seibersdorf, Austria.
[b]Also at: Department of Physics and Astronomy, University of Iowa, Iowa.
[c]Also at: LPMI URA 835, Université Henri Poincaré, Nancy, France.

 © 2000 American Institute of Physics

Downloaded 21 Sep 2000 to 192.93.241.42.Redistribution subject to AIP copyright, see http://ojps.aip.org/pop/popcpyrts.html.

rection representing the radial direction. The 1-D Vlasov equation for the main ions' distribution function $f_i(y,v_x,v_y,v_z)$ is written:

$$\frac{\partial f_i}{\partial t}+v_y\frac{\partial f_i}{\partial y}+\frac{e}{m_i}(\mathbf{E}+\mathbf{v}\times\mathbf{B})\cdot\frac{\partial f}{\partial \boldsymbol{\nu}}=0 \tag{1}$$

with a similar equation for the impurity distribution function f_I, with the subscript ''I'' replacing the subscript ''i'' in Eq. (1) **B** denotes the constant magnetic field situated in the (x,z) plane, and makes an angle $\theta=89°$ with the x axis (z represents the periodic toroidal direction and x represents the periodic poloidal direction, which are considered homogeneous in the present calculation). **v** is the velocity and the electric field **E** is calculated from

$$\mathbf{E}=-\nabla\varphi, \tag{2}$$

where the potential φ is calculated from Poisson's equation (for singly ionized impurity ions $Z=1$):

$$\Delta\varphi=-4\pi e(n_i+n_I-n_e) \tag{3}$$

and $n_{i,I}=\int f_{i,I}\,d\mathbf{v}$. The electron density n_e is calculated from an adiabatic law,

$$n_e=n(y)e^{e\varphi/T_e}. \tag{4}$$

As we mentioned in Sec. I, we are calculating a charge separation in a non-neutral plasma along a gradient where the electron density changes rapidly over an ion orbit size, and the electrons cannot exactly compensate the ions charge along the gradient. This charge separation is calculated on the Debye length scale, which is assumed small but finite. Hence the importance of calculating the potential from the Poisson equation.

We normalize time to ω_{pi}^{-1}. Velocity is normalized to the acoustic velocity $C_s=\sqrt{T_e/m_i}$, and length is normalized to $C_s\omega_{pi}^{-1}$. The potential is normalized to T_e/e. We take as initial density

$$n(y)=0.5(1+\tanh(y/15)) \tag{5}$$

in the domain $-80<y<80$.

The initial distribution function for the main ions is given by

$$f_i(y,\mathbf{v})=n_i\frac{1}{2\pi T_{i0}}e^{-(v_x^2+v_y^2)^2/2T_{i0}}\frac{1}{(2\pi T_i(y)^{1/2}}e^{-v_z^2/2T_i(y)}. \tag{6}$$

A similar expression is used for the impurity ions' distribution $f_I(y,\mathbf{v})$. Temperature is assumed constant (T_{i0}) in the direction almost perpendicular to the magnetic field, and having a profile $T_i(y)$ in the direction almost parallel to the magnetic field. This is done to keep our initial conditions close to what was presented in Ref. 1, since the averaging over the gyro-motion was effected with a constant temperature in the direction normal to the magnetic field. Also, during the evolution of the system, the gyration around the magnetic field has a tendency to evolve the temperature to a constant value in the direction perpendicular to the magnetic field.

The relevant physical parameters, in dimensionless form, are chosen as follows:

$$T_e/T_{i0}=1,\quad m_i/m_e=1840,\quad \omega_{ci}/\omega_{pi}=0.1,\quad m_I/m_i=10 \tag{7}$$

and the ratio of the ion gyroradius to the Debye length is given by

$$\rho_i/\lambda_{\mathrm{De}}=\frac{v_{ti}/\omega_{ci}}{\lambda_{\mathrm{De}}}=\frac{\sqrt{T_{i0}/T_e}}{\omega_{ci}/\omega_{pi}}=10. \tag{8}$$

The numerical code uses a method of fractional steps associated with cubic spline interpolation, similar to what has been used in Ref. 1. This method has proven through many applications to give accurate results (see Ref. 2). We use a time step $\Delta t=0.1$. The computational domain is $-80<y<80$, $-4<v_x<4$, $-4<v_y<4$, $-4<v_z<4$. The number of grid points is $N_yN_{vx}N_{vy}N_{vz}=160\times50\times50\times50$. Our simulation was performed with $\theta=89°$ (the magnetic field is almost in the toriodal z direction, with a small component in the periodic poloidal x direction), and with a temperature profile for the distribution in v_z, as indicated in Eq. (6):

$$T_i(y)=T_{i0}(0.2+0.4(1+\tanh(y/10))) \tag{9}$$

with $T_{i0}=T_e=1$, and $T_I(y)=T_i(y)$ for the impurity ions. In the parameters presented, we have kept the parameters as close as possible to what has been presented in Ref. 1.

III. RESULTS WITH A SINGLE ION SPECIES

In this first simulation, we use $n_i=n(y)$ [given in Eq. (5)], and $n_I=0$ with the profiles chosen in Eqs. (5), (6), and (9). The code shows an initial oscillation with an initial buildup of the potential φ at the edge (see Fig. 1), reaching a peak at $t=30$, decaying, then again reaching another peak at $t=85$. This corresponds to a period of about 55 or 56 (in our units where time is normalized to ω_{pi}^{-1}, the gyro-period is $t=2\pi/\omega_{ci}=62.8$). Then the oscillation repeats itself with the same period. Note that during the oscillation, as the main potential peak is decaying, a second peak, coming from behind from inside the plasma, is growing until it dominates and generates the main peak at the maximum. Note also, as the oscillation progresses in time, the minimum of the potential building up to the point where the difference between the maximum and the minimum profiles is small, and the oscillation takes the form of a constant pulsation of the potential profile. The potential builds up an important structure with a potential profile with a strong positive bump near the edge (see the results from $t=945$ to $t=995$). Figure 2 shows the electric field profile, which is rapidly building up a shape with a positive bump in the center, confining the ions to the right. This electric field oscillates with the potential, but always keeps a small positive bumpy structure in the center as we advance in time, as we see from Fig. 2. The electric field profile in Fig. 2 decays to a negative value at the edge, where we have fixed the potential equal to zero at the left boundary. Note, as time advances, the almost constant decay of the electric field at the edge, while behind the edge to the interior the wavy structure of the field with an oscillation which gives the appearance of being generated at the right, inside the plasma, where the potential is zero, and propagating to the left. Note during a period of oscillation, for instance from

Downloaded 21 Sep 2000 to 192.93.241.42.Redistribution subject to AIP copyright, see http://ojps.aip.org/pop/popcpyrts.html.

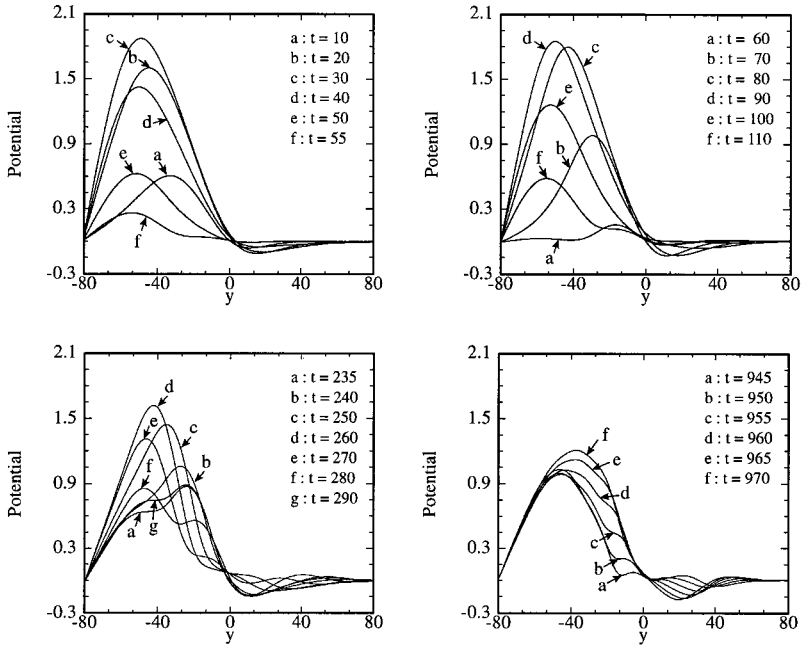

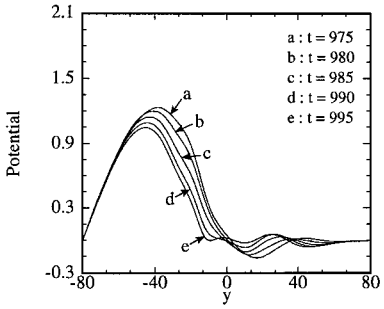

FIG. 1. Potential profile at different times for the case without impurity ions.

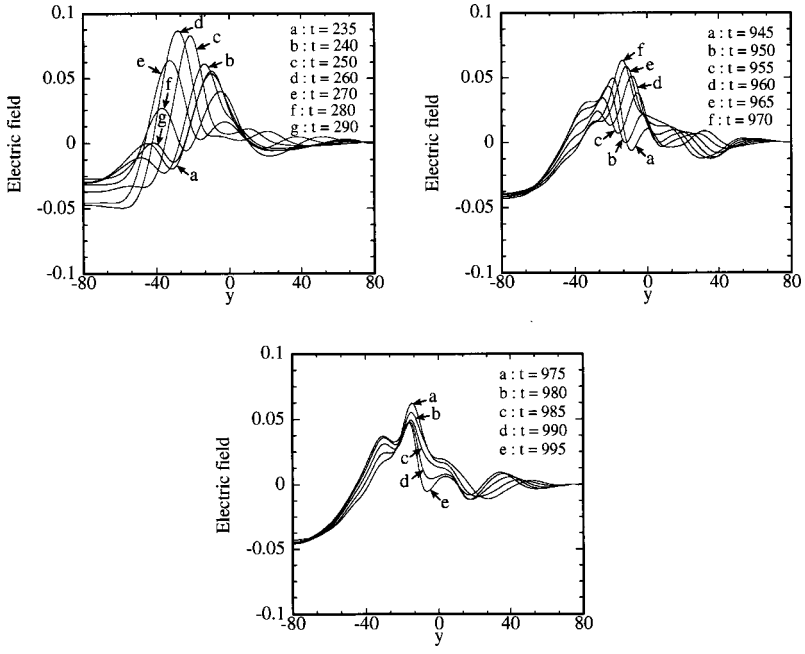

FIG. 2. Electric field profile E_y at different times for the case without impurity ions.

Downloaded 21 Sep 2000 to 192.93.241.42.Redistribution subject to AIP copyright, see http://ojps.aip.org/pop/popcpyrts.html.

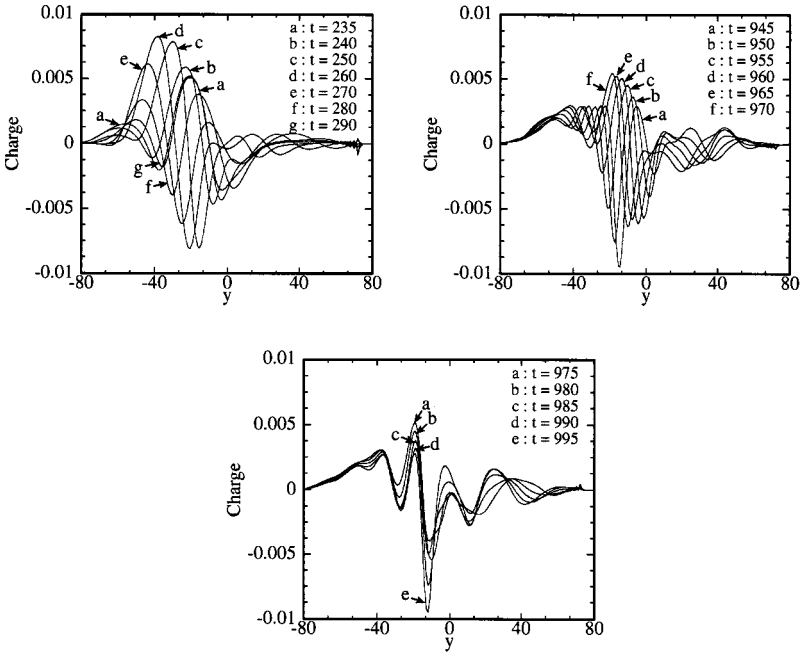

FIG. 3. Charge $(n_i - n_e)$ at different times for the case without impurity ions.

$t=945$ to $t=995$, the electric field at the very edge remaining nearly constant, in spite of the wavy profile which oscillates in time behind the edge. Note during the first half of the oscillation, for instance from $t=945$ to $t=970$, the pulse coming from the inside with the peak which seems to propagate toward the edge. This is followed during the second half of the oscillation cycle, from $t=975$ to 995, by the peaks decaying or growing at almost the same position, a picture close to a standing wave. Note also a similar pattern in the time evolution of the potential, with the slope at the edge of the corresponding potential profile in Fig. 1 remaining essentially constant (see the results from $t=945$ to 995). During the first half of the oscillation cycle from $t=945$ to $t=970$, there is a pulse-like structure going up-hill on the negative slope of the potential bump until it reaches the peak, while during the second half-period of the oscillation, from $t=975$ to 995, the pulsation on the negative slope side of the potential bump seems to collapse to the minimum at $t=995$. The same pattern of oscillation appears in the evolution of the charge in Fig. 3. The difference $n_i - n_e$ is the charge contribution to Eq. (3), and Fig. 3 shows the charge $n_i - n_e$ at different times. This charge is relatively small (of the order of 10^{-3}), and it is this small difference between n_i and n_e which, for large values of ρ_i/λ_{De}, and in the presence of a density gradient, translates into an important contribution in the calculation of the potential (see the discussion in Ref. 1).

Figure 4 shows the ion density profile during different periods of the charge oscillation, during the period from $t=680$ to 730, for instance. It shows how the gradient slowly oscillates in time. See during the first half of the oscillation (for instance, from $t=840$ to 865) when the charge pulse is propagating to the left, the density profile collapsing slowly from the top, while during the second half of the oscillation (from $t=870$ to $t=885$, for instance), the top of the density plateau reforming itself, then collapsing again from $t=895$ to $t=920$. Note the persistent oscillation until the end, keeping essentially the same period as at the beginning. The electron density profile calculated from Eq. (4) shows the same profile as in Fig. 4 (since the charge $n_i - n_e$ of the order of 10^{-3}).

IV. RESULTS OBTAINED WITH IMPURITY IONS

We repeat the simulation presented in Sec. III by adding a small fraction of impurity ions, to show the effect of a small fraction of impurity ions on the rapid buildup of the potential and electric field. We use parameters similar to what has been presented in Ref. 1. We use for the initial impurity density profile $n_I = 0.05n(y)$, where $n(y)$ is defined in Eq. (5). We use for the main ion species $n_i = 0.95n(y)$, i.e., we have 5% impurity ions. So the main ions' and the impurity ions' profile decay initially in a similar way toward the edge. We assume a temperature profile for the impurity ions $T_I(y) = T_i(y)$, where $T_i(y)$ is defined in Eq. (9). We also assume that the impurity ions are singly ionized $(Z=1)$, and $m_I/m_i = 10$. We use for the impurity ions another set of equations similar to Eqs. (1) and (6) for the impurity ions' distribution function $f_I(y, v_x, v_y, v_z)$.

Initially, we have $n_i + n_I = n(y)$. The results show initially the development of an oscillation similar to what has been presented in Sec. III. In fact, during the first period of the oscillation, the evolution of the potential, the charge, and the electric field are *identical* to what has been presented in Fig. 1 during the first period of the oscillation. The main ions, evolving more rapidly than the heavy impurity, adjust themselves initially so that the total ion density $n_i + n_I$, initially equal to $n(y)$ at $t=0$, remains identical to the density n_i obtained in the simulation presented during the first period of oscillation in the results of Sec. III. It results that the charge $n_i + n_I - n_e$, and consequently the potential and the electric field, are identical during the first period of oscilla-

Downloaded 21 Sep 2000 to 192.93.241.42.Redistribution subject to AIP copyright, see http://ojps.aip.org/pop/popcpyrts.html.

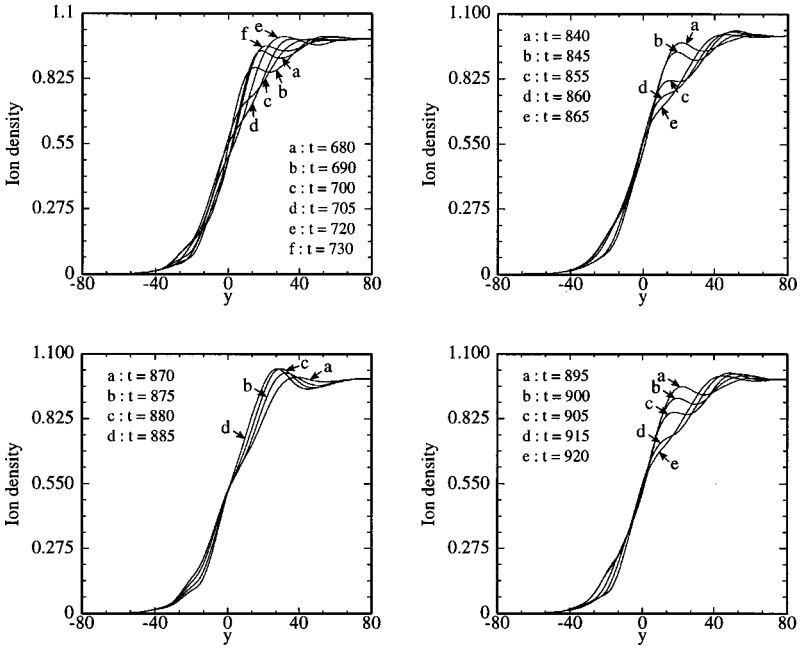

FIG. 4. The ion density profile at different times for the case without impurity ions.

tions to the equivalent ones in Sec. III. The impurity ions, however, with a larger gyroradius diffuse more rapidly to the outside (to the left of the space domain in the figure) than the main ion species. In Fig. 5, we see how the impurity ions' density extends toward the left, adding a positive charge in a region which cannot be reached by the smaller gyroradius main ion species, which are effectively pushed back by the electric field than the heavy impurity ions. This results in a positive charge accumulation at the edge due essentially to the contribution of the small fraction of impurity ions. Figure 6 shows the potential at different times. At $t=240$, for instance, we see how the minimum potential for the present results with impurity ions is more important than the corresponding one presented in Fig. 1. Figures 7 and 8 show the electric field and the charge, respectively, where the charge for the present simulation is $(n_i+n_I-n_e)$. The curves in Fig. 8 show in the present simulation an accumulation of a positive charge at the edge resulting from the impurity ions, while the remaining charge toward the center remains close to what has been presented in Sec. III. The electric field presented in Fig. 7 indicates an increase in the electric field in the present simulation at the very edge with respect to the results obtained in Sec. III. However, with $m_I/m_i=10$, the gyro-period of the impurity ions is around 560 (since for the main ion species the gyro-period is 56 in our units). This double periodicity of the main species and the impurity ions (56 and 560, respectively) has its signature in the results. We present in Fig. 9 the time evolution of the potential (full curve) and the charge (dotted curve, multiplied by a factor of 20) monitored at the position $y=-40$ (around the maximum of the potential), and the electric field (a broken curve multiplied by a factor of 10) monitored at the position $y=-15$ (around the maximum of the positive bump of the electric field). The beating of the two periods of gyration is apparent in Fig. 9. there is a big peak in the potential due to the impurity ions rushing to the edge at $t=150$, followed by another peak around $t=720$. On this is superimposed the main ions gyro-period of about 56. We show in Fig. 10 the potential profile at the peak at $t=720$ (curve b), to be compared with the corresponding one from Sec. III (curve a). The gyration of the impurity ions brings another peak around $t=710$, increasing the positive charge accumulation at the edge, together with the electric field and the potential (see the impurity ions' density extending to the edge in Fig. 5). Note, however, that the difference in the profiles in Figs. 10–12 appears essentially for $y<-40$. For $y>-40$, the profiles remain close. This means in the present case that in the calculation of the charge $n_i+n_I-n_e$, the total contribution

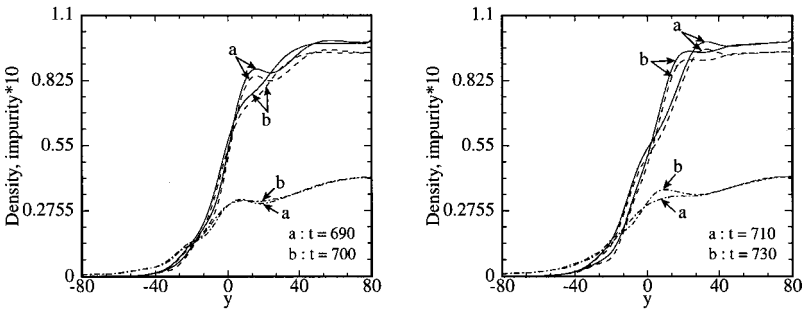

FIG. 5. The density profiles at different times. The full curve is for the electrons. Main ions and impurity ions are in broken curves. The scale of the impurity ions is multiplied by 10.

Downloaded 21 Sep 2000 to 192.93.241.42.Redistribution subject to AIP copyright, see http://ojps.aip.org/pop/popcpyrts.html.

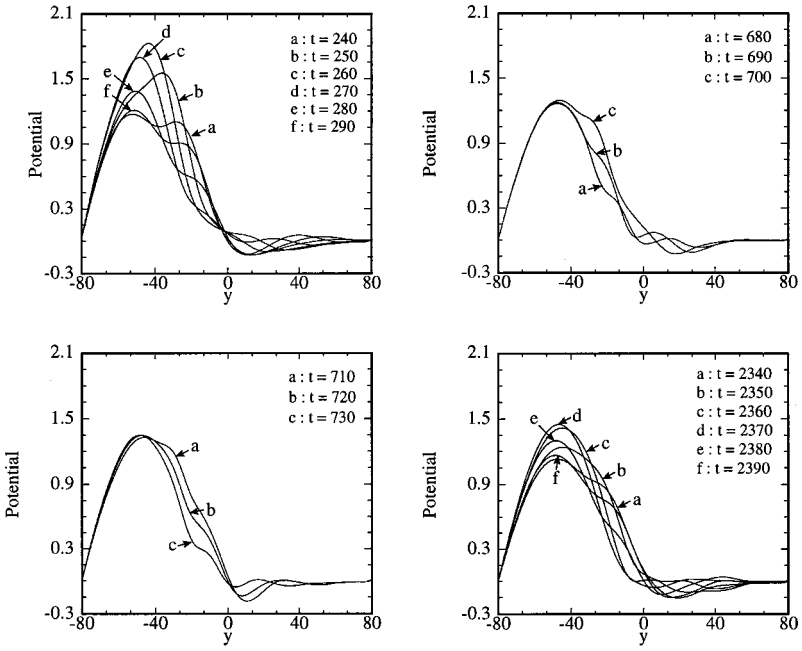

FIG. 6. Potential profiles at different times for the case with impurity ions.

$n_i + n_I$ must be very close for $y > -40$ to the ion contribution n_i calculated in Sec. III, since the charge presented in Fig. 12 at $t = 720$ is essentially the same for $y > -40$. Around $t = 2390$, the impurity ions have already executed around five gyrations. There is an almost constant profile of the charge, electric field, and potential at the very edge of the plasma, and the pattern of the oscillations is still appearing coming from behind the edge. This oscillation pattern, which appears as coming from the interior and damping at the edge, is now the complicated combination of the main ion gyration and the impurity ions' gyration. We present in Figs. 6–8 a complete cycle of these from $t = 2340$ to $t = 2390$. The electric field at the very edge is at least 50% higher with respect to what has been obtained in Sec. III without impurity ions.

Finally, we show in Figs. 13–15 the contour plots of the following functions:

$$F_i(y,v_y) = \int_{-\infty}^{\infty}\int_{-\infty}^{\infty} f_i(y,v_x,v_y,v_z)dv_x\, dv_z, \tag{10}$$

$$F_i(y,v_x) = \int_{-\infty}^{\infty}\int_{-\infty}^{\infty} f_i(y,v_x,v_y,v_z)dv_y\, dv_z \tag{11}$$

with similar plots for the impurity distributions $F_I(y,v_y)$ and $F_I(y,v_x)$.

In Fig. 13 the contour plots of $F_i(y,v_y)$ is presented at $t = 2370$ (around one of the peaks of the potential in Fig. 9). We see from Fig. 13 how the positive bump of the electric

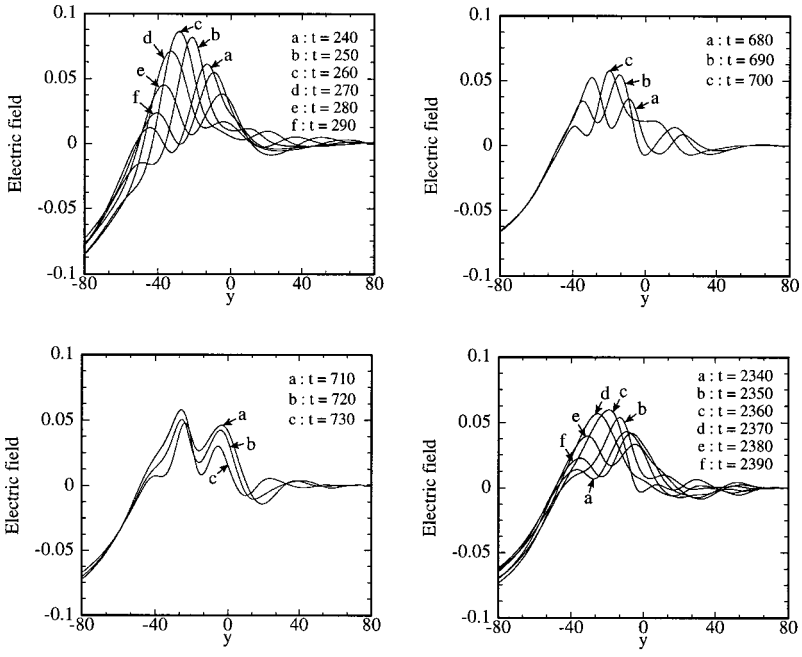

FIG. 7. Electric field profiles at different times for the case with impurity ions.

Downloaded 21 Sep 2000 to 192.93.241.42.Redistribution subject to AIP copyright, see http://ojps.aip.org/pop/popcpyrts.html.

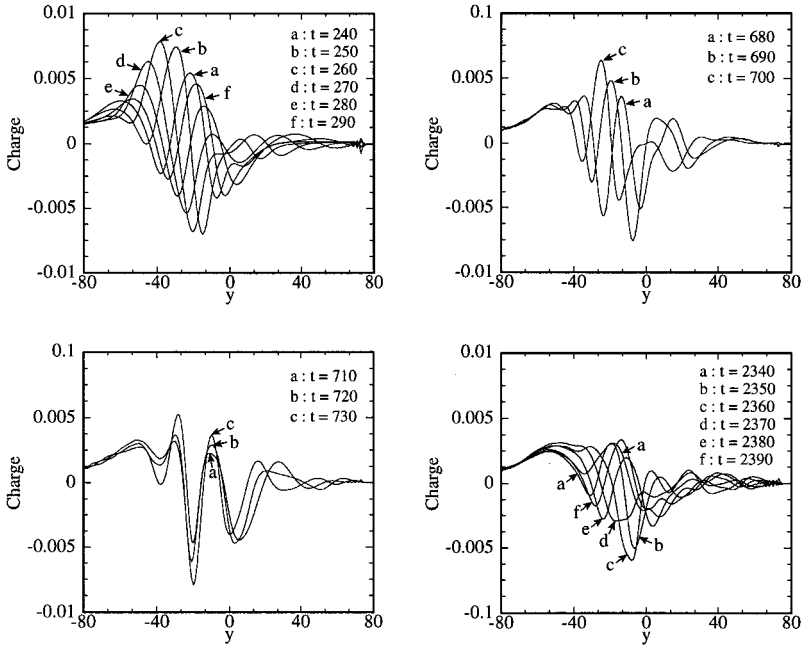

FIG. 8. Charge profiles ($n_i+n_I-n_e$) at different times for the case with impurity ions.

field is pushing the main ion species away from the edge. Figure 14 presents the corresponding impurity ions' distribution $F_I(y,v_y)$ calculated from $f_I(y,v_x,v_y,v_z)$ as indicated in Eq. (10), at $t=2380$. Note how the impurity ions extend to the left boundary, providing a positive charge in a region the main ion species are not reaching, prevented by the positive part of electric field. A contour plot of the distribution function $F_i(y,v_x)$ [see Eq. (11) for the main ion species] is presented in Fig. 15 at $t=2370$. The corresponding contour plot of the impurity ions' distribution $F_I(y,v_x)$ is given in Fig. 16. The distribution functions in Figs. 13–16 are those close to the perpendicular direction of the magnetic field and are not Maxwellian. It is clear that the resulting effect of the electric field with the gyration in velocity space across the magnetic field will generally distort the distribution functions from a Maxwellian. In the present normalization, the thermal ions gyroradius is 10 length units for the present parameters. The impurity gyroradius (with $m_I/m_i=10$) is about 30. This is close to the scale length of the electrostatic potential bump calculated. We are certainly in a regime where the exact orbit integration in the self-consistent field using the fully kinetic code is necessary, and the validity of the gyro-kinetic equations to describe these large gyro-orbit ions and impurities could be at best approximate. The gyro-kinetic equations used in Ref. 1 are averaged over the ion gyration assuming a Maxwellian distribution in the direction perpendicular to the magnetic field, with constant temperature. The results we present may be qualitatively close to the results presented in Ref. 1 for the present set of parameters (within a factor of about 2), without necessarily implying that this will always be the case and for other sets of parameters, and that all the assumptions used in the derivation of the gyro-kinetic equa-

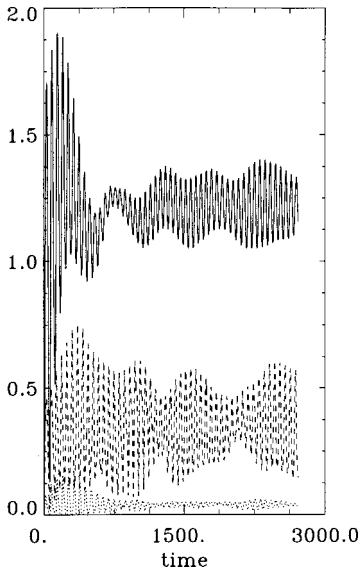

FIG. 9. Time evolution of the potential and the charge monitored at the position $y=-40$ (charge is multiplied by a factor of 20), and the electric field (monitored at the position $y=-15$, multiplied by a factor 10) for the case with impurity ions.

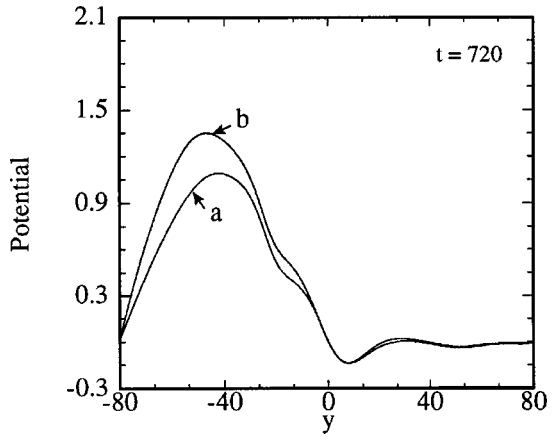

FIG. 10. Potential profiles at $t=720$ for (a) the case without impurity ions, (b) the case with impurity ions.

Downloaded 21 Sep 2000 to 192.93.241.42.Redistribution subject to AIP copyright, see http://ojps.aip.org/pop/popcpyrts.html.

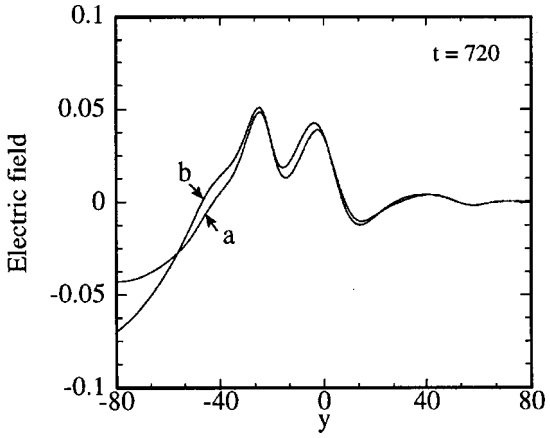

FIG. 11. Electric field profiles E_y at $t=720$ for (a) the case without impurity ions, (b) the case with impurity ions.

tions presented in Ref. 1 are necessarily fulfilled. However, the present results, calculated with the same parameters as in Ref. 1, offer a useful indication on how good the gyrokinetic approximation used in Ref. 1 is for the present problem and set of parameters, and for the present distortion of the distribution functions.

V. CONCLUSIONS

With a time step $\Delta t=0.1$, we have followed for more than 27 000 time steps, for the case with impurity ions presented in Sec. IV, the formation and the evolution of a charge separation of the order of 10^{-3}, together with the self-consistent electric field and potential, in the presence of a density gradient at a plasma edge. The formation of the charge separation and the electric field at the edge of the plasma results from the fact that due to the finite ion gyroradius, the electrons cannot exactly compensate the ion charge along the gradient. We have shown that the presence of a small fraction of impurity ions (5% in the present simulation, with $m_I/m_i=10$) at the plasma edge can have a significant effect in the more rapid buildup and increase of the charge and the associated electric field at the edge, in comparison to the case when no impurity ions were included (the

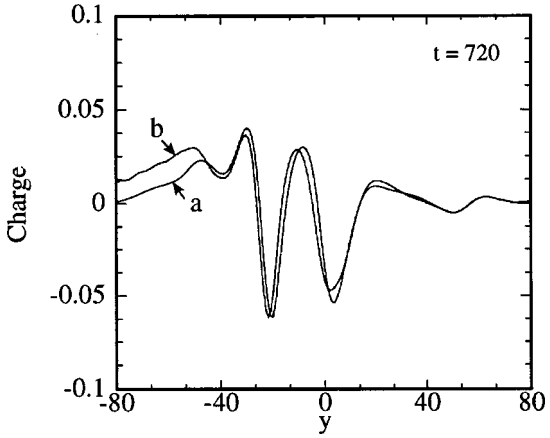

FIG. 12. Charge profiles $(n_i+n_I-n_e)$ at $t=720$ for (a) the case without impurity ions, (b) the case with impurity ions.

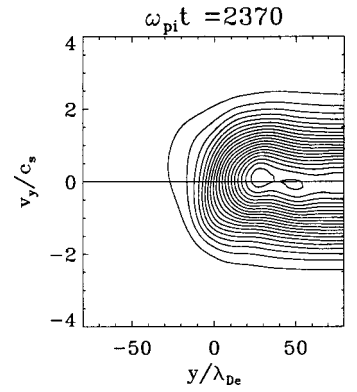

FIG. 13. Contour plot of $F_i(y,v_y)$ for the main ions at $t=2370$.

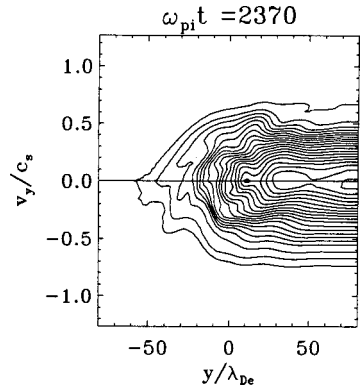

FIG. 14. Contour of $F_I(y,v_y)$ for the impurity ions at $t=2370$.

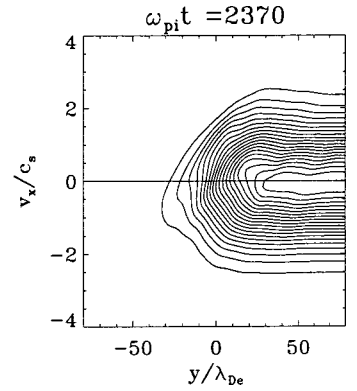

FIG. 15. Contour plot of $F_i(y,v_x)$ for the main ions at $t=2370$.

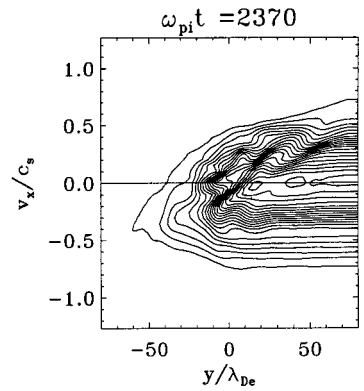

FIG. 16. Contour plot $F_I(y,v_x)$ for the impurity ions at $t=2370$.

Downloaded 21 Sep 2000 to 192.93.241.42.Redistribution subject to AIP copyright, see http://ojps.aip.org/pop/popcpyrts.html.

impurity ions have been assumed to have a similar profile shape as the main ion species in the present simulation; however, impurity can usually be more concentrated at the edge, and consequently gives a more effective contribution to the edge positive charge). The potential and electric field created are increasing along the gradient. The electric field reaches a peak on the low side of the gradient, and the potential is reaching a peak further away, in front of the gradient. We have also shown that in the presence of a gradient, there are oscillations at the edge which are closely related to the gyration of the ions.

We have followed the evolution of periodic oscillations at the plasma edge due to the ions' gyro-motion. For a magnetic field of 2 T, this corresponds to a period of 10^{-8} s. Edge localized modes (ELMs) are oscillations appearing at the tokamak edge. A typical period of oscillation of ELMs will be around 10^{-3} s. We have pointed to the strong dependence of the effective charge at the edge on the parameter ρ_i/λ_{De}. During the poloidal rotation of the edge plasma, this parameter is strongly modulated due to the variation of the toroidal magnetic field. This strong modulation of ρ_i/λ_{De} during the poloidal rotation of the edge translates into a strong modulation of the effective charge and potential, which can certainly be associated with the ELMs (edge localized modes). For the results reported for TdeV (Tokamak de Varennes), for instance,[7] the poloidal velocity of the edge at the separatrix is about 2.2 km/s. The minor radius is about 0.22 m. This translates into an average period of poloidal rotation of about $2\pi\times 0.22/2200\approx 0.6\times 10^{-3}$ s.

There is experimental evidence[4,8] of increased poloidal rotation at a plasma edge with the injection of impurity ions. In the present simulation, we have used $m_I/m_i=10$. In practical experimental situations, this ratio can be much bigger (krypton was used in the results presented in Ref. 8), which will result in a larger gyroradius. The importance of large gyroradius impurity ions in creating a charge at a plasma edge has also been recently pointed out in Ref. 9. What appears in the present simulation as a small positive bump of the electric field at the edge can in practice be more important. In addition, many impurities can be present at the edge. Friction with neutrals and other collisions at the edge can also play a very important role in the physics of the present problem. As pointed out in Ref. 10, for ions with charge number $Z\geqslant 2$, a random walk diffusion can be caused by the fluttering of the gyroradius as a result of successive recombination and ionization events. Neutral impurities are subjected to transport across the magnetic field due to their unimpeded motion during the short atomic phases. The importance of charge exchange events with cold neutral atoms has been recently noted in Ref. 11. Poloidal asymmetry of the impurity density, which occurs because of the rotation, results in an enhancement of diffusivity.[12] All these effects will add to a diffusion which will further widen what is presented in the present simulation as a small positive bump in the electric field profile. We can speculate that this electric field will have an important effect on what is usually called the transport barrier, and will result in new transport effects at the edge which are neither neoclassical nor anomalous.

The physics of the charge separation at a plasma edge is important not only in tokamak physics. For instance, the existence of a shear layer at the edge of the reversed field experiment has been recently reported,[13] with a shearing rate level comparable to tokamaks in the high-confinement mode (H mode). Also, similar results were reported in toroidal helical plasma.[14]

It is beyond the scope of the present work to discuss cylindrical geometry effects on the present results. We note, however, that these effects could be relevant in studying the charge separation at a plasma edge.[15]

Finally, we note that the region of the divertor in a tokamak is a region rich with impurities and cold neutral atoms, in which friction due to charge exchange can be important. In view of the present results, one expects an important electric field to be present in this region, an one expects that this electric field will play an important role in the divertor region, especially in what is called a detached plasma regime.

The present results show the power and the importance of the Eulerian Vlasov codes, which with their low noise level offer a powerful tool for the study of these problems.

ACKNOWLEDGMENTS

The Centre Canadien de Fusion Magnétique is funded by Hydro-Québec and by the Institut National de la Recherche Scientifique.

[1] M. Shoucri, E. Pohn, G. Knorr, P. Bertrand, G. Kamelander, G. Manfredi, and A. Ghizzo, Phys. Plasmas **6**, 1401 (1999).
[2] C. Cheng and G. Knorr, J. Comput. Phys. **22**, 330 (1976); M. Shoucri and R. Gagné, *ibid.* **27**, 315 (1978).
[3] B. Coppi, H. P. Furth, M. N. Rosenbluth, and R. Z. Sagdeev, Phys. Rev. Lett. **17**, 377 (1966).
[4] B. Coppi, *Proceedings of the 13th International Conference on Plasmas Physics and Controlled Fusion, Washington DC, 1990* (International Atomic Energy Agency, Vienna, 1990), Vol. 2, p. 413.
[5] See, for instance, the JET Team, paper presented by C. Gormezano, ''High performance with modified shear in JET D-D and D-T plasmas,'' Proceedings of the 17th International Conference on Plasmas Physics and Controlled Fusion, Japan, 1998 (International Atomic Energy Agency, Vienna, to be published); R. Weynants, *ibid.* ''Overview of RI-Mode results on Textor—94.''
[6] M. Shoucri, E. Pohn, P. Bertrand, G. Knorr, G. Kamelander, G. Manfredi, and A. Ghizzo, in *Proceedings of the 26th EPS Conference on Controlled Fusion and Plasma Physics, Maastricht, 1999* (European Physical Society, Petit-Lancy, 1999).
[7] I. Condrea, E. Haddad, B. Gregory, D. Lafrance, J.-L. Lachambre, G. Pacher, F. Meo, and H. Mai, Rev. Sci. Instrum. **70**, 387 (1999).
[8] D. Pacella, B. Gregory, M. Leigheb, G. Pizzicaroli, G. Mazzitelli, M. Borra, L. Pieroni, M. May, K. Fournier, W. Goldstein, M. Finkental, M. Mattioli, and the FTU Team, in *Proceedings of the 25th EPS Conference on Controlled Fusion and Plasma Physics, Prague, 1998* (European Physical Society, Petit-Lancy, 1998).
[9] R. Bartiromo, Phys. Plasmas **5**, 3342 (1998).
[10] G. Fussman, Contrib. Plasma Phys. **37**, 363 (1997); P. Helander, S. Krasheninnikov, and P. J. Cato, Phys. Plasmas **1**, 3174 (1994).
[11] P. Monier-Garbet, K. H. Burrell, F. L. Hinton, J. Kim, X. Garbet, and R. J. Groebner, Nucl. Fusion **37**, 403 (1997).
[12] M. Romanelli and M. Ottaviani, Plasma Phys. Controlled Fusion **40**, 1767 (1998).
[13] V. Antoni, D. Desideri, E. Martines, G. Serianni, and L. Trancontin, Phys. Rev. Lett. **79**, 4814 (1997).
[14] A. Fujisawa, H. Iguchi, T. Minami *et al.*, Phys. Rev. Lett. **82**, 2669 (1999).
[15] B. Krane, I. Christopher, M. Shoucri, and G. Knorr, Phys. Rev. Lett. **80**, 4422 (1998).

Downloaded 21 Sep 2000 to 192.93.241.42.Redistribution subject to AIP copyright, see http://ojps.aip.org/pop/popcpyrts.html.